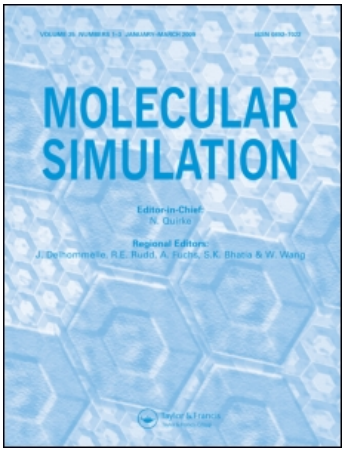

Molecular Simulation
Publication details, including instructions for authors and subscription information:
http://www.informaworld.com/smpp/title~content=t713644482

Molecular dynamics simulations of the incorporation of Mg 2+ , Cd 2+ and Sr 2+ at calcite growth steps: Introduction of a SrCO 3 potential model

N. H. de Leeuw[a]; J. H. Harding[b]; S. C. Parker[c]
[a] Department of Chemistry, University of Reading, Reading, UK [b] Department of Physics and Astronomy, University College London, London, UK [c] Department of Chemistry, University of Bath, Bath, UK

Online publication date: 26 October 2010

To cite this Article de Leeuw, N. H. , Harding, J. H. and Parker, S. C.(2002) 'Molecular dynamics simulations of the incorporation of Mg 2+ , Cd 2+ and Sr 2+ at calcite growth steps: Introduction of a SrCO 3 potential model', Molecular Simulation, 28: 6, 573 — 589
To link to this Article: DOI: 10.1080/08927020290030143
URL: http://dx.doi.org/10.1080/08927020290030143

Molecular Simulation, 2002 VOL. 28 (6-7), pp. 573–589

MOLECULAR DYNAMICS SIMULATIONS OF THE INCORPORATION OF MG^{2+}, CD^{2+} AND SR^{2+} AT CALCITE GROWTH STEPS: INTRODUCTION OF A $SRCO_3$ POTENTIAL MODEL

N.H. DE LEEUW[a,*], J.H. HARDING[b] and S.C. PARKER[c]

[a]*Department of Chemistry, University of Reading, Whiteknights, Reading RG6 6AD, UK;* [b]*Department of Physics and Astronomy, University College London, Gower Street, London WC1E 6BT, UK;* [c]*Department of Chemistry, University of Bath, Claverton Down, Bath BA2 7AY, UKUK*

(Received April 2001, accepted August 2001)

Molecular dynamics simulations were used to model the incorporation of magnesium, cadmium and strontium ions at two stepped $(10\bar{1}4)$ surfaces of the calcium carbonate polymorph calcite. The potential model used in the simulations was derived to reproduce experimental enthalpies of $CaCO_3$, $MgCO_3$, $CdCO_3$ and $SrCO_3$ formation and dissolution and the effect of solvent was modelled by the addition of a layer of water molecules. From the calculated energies we expect that, in a solution containing all four cations, $MgCO_3$ and $SrCO_3$ grow onto the calcite steps in preference to $CdCO_3$ and especially $CaCO_3$. Growth of complete rows of $MgCO_3$ and $CdCO_3$ occurs at either step edge, while growth of a row of $SrCO_3$ at the acute edge releases a large amount of energy ($-420\,kJ\,mol^{-1}$), which should, therefore, be the preferential step for incorporation of complete $SrCO_3$ edges.

Keywords: Calcite; Computer simulation; Impurities; Growth; Inhibition

INTRODUCTION

Calcite is one of the most abundant minerals in the environment and of fundamental importance in many fields, both inorganic and biological. It is a building block of shells and skeletons [1] and is used as a carbon isotope counter

*Corresponding author. E-mail: n.h.deleeuw@reading.ac.uk.

ISSN 0892-7022 © 2002 Taylor & Francis Ltd
DOI: 10.1080/08927020290030143

in marine carbonates, with a view to assessing the relationship between the CO_2-induced greenhouse effect and climate [2]. Furthermore, calcium carbonate is important in ion exchange, due to its strong surface interactions with heavy metals in the environment [3,4], in energy storage where the products of its endothermic decomposition into CaO and CO_2 can be stored and subsequently reacted exothermically to re-release the energy [5] and in industrial water treatment [6]. Hence, calcite has been the subject of extensive and varied research. One area of research which has attracted much attention is crystal growth and dissolution, e.g. [7–10]. As the concentration of calcium carbonate in many natural waters exceeds the saturation level, the precipitation of calcite in industrial boilers, transportation pipes and desalination plants is of concern [11] and it is, therefore, important to learn how crystal growth and dissolution are affected and can be modified.

The $(10\bar{1}4)$ surface is by far the most stable plane of calcite and dominates the observed morphology [12–14]. Hence, it has been the subject of many investigations, both in ultra-high vacuum such as the SEM study by Goni *et al*. [15], in air [16] and under aqueous conditions such as the AFM investigations by Ohnesorge and Binnig [17] and Liang *et al*. [18]. However, no experimental surface is truly planar and there are always defects present such as steps and kinks. Indeed, calcite growth and dissolution is found to occur through steps [19] and spiral dislocations [20], often in monolayers from the step as observed by Liang *et al*. [18] in their AFM study of the calcite $(10\bar{1}4)$ plane under aqueous conditions and by Stipp *et al*. [16] who used SFM to study the same surface in air over some days and found the steps to spread one layer at a time. Side reactions, such as the oxidation of pyrite and ammonia, often affect the rate of $CaCO_3$ dissolution [21]. Recent models of step dissolution have included a terrace–ledge–kink model, successfully describing the initial stages of pit growth on the $\{10\bar{1}4\}$ surface [22,23], a kinetic Monte Carlo model which reproduces experimental pit-growth behaviour [24] and molecular dynamics simulations, comparing dissolution of calcium carbonate units from two experimentally observed step edges, which correctly calculated the preference of dissolution from one particular step [25].

Many impurity ions are found to affect crystal growth, e.g. Compton and Brown [26] who showed that magnesium ions inhibit calcite growth and, hence, studies of crystal growth have often concentrated on the effect of incorporating into the crystal foreign ions such as copper and manganese [27], iron [28] and other divalent cations [26,29,30], phosphate species [6,31] or organic matter [32–34]. Earlier computational studies [35,36] have confirmed experimental findings [37] that lithium and HPO_4^{2-} impurities radically change the morphology of calcite, and predicted that magnesium ions would do likewise. Foreign ions can

be incorporated at the growing steps, e.g. boron oxyanions [38] and atomistic simulation methods have been used to model growth inhibition by incorporation of diphosphates into the steps [39].

The aim of the work described in this paper is to use molecular dynamics simulations to investigate the energetics of the uptake of magnesium, cadmium and strontium ions into the growing calcite crystal. Magnesium, cadmium and strontium are all found as impurity ions in calcite, especially magnesium, which forms a complete solid solution with calcium from the purely isomorphous magnesium phase magnesite, through dolomite, which has an ordered 50/50 mixture of magnesium and calcium, to pure calcite [40]. The simulation of impurity uptake into the crystal is achieved by modelling the growth of $MgCO_3$, $CdCO_3$ and $SrCO_3$ units onto two experimentally observed monatomic steps on the calcite $10\bar{1}4$ surface. As crystal growth occurs under aqueous conditions, we have included solvent effects in the simulation by modelling the growth process in the presence of water molecules.

THEORETICAL METHODS

The energies of incorporation of magnesium, cadmium and strontium ions at the calcite surfaces were calculated using classical molecular dynamics simulations. These methods are based on the Born model of solids [41] which assumes that the ions in the crystal interact via long-range electrostatic forces and short-range forces, including both the repulsions and the van der Waals' attractions between neighbouring electron charge clouds, which are described by simple analytical functions. The electronic polarisability of the ions is included via the shell model of Dick and Overhauser [42] in which each polarisable ion, in our case the oxygen ion, is represented by a core and a massless shell, connected by a spring. The polarisability of the model ion is then determined by the spring constant and the charges of the core and shell. When necessary, angle-dependent forces are included to allow directionality of bonding as, for example, in the model of the covalent carbonate anion developed by Pavese *et al*. [42].

The computer code used for the molecular dynamics simulations was DL_POLY 2.9 [43]. To obtain the necessary data on bulk liquid water we simulated a box containing 256 water molecules at a temperature of 300 K. The equilibration of the water simulation cell was achieved by initially setting the experimental density of $\rho = 1.0\,\mathrm{g/cm^3}$ and using NVE (constant number of particles, volume and energy), NVT (constant number of particles, volume and temperature) and NPT (constant number of particles, pressure and temperature) ensembles in sequence. The final data collection simulations were run at NPT.

The energies of the aqueous ions were calculated using a simulation cell containing 255 water molecules plus the cation or carbonate group. The simulation cell was equilibrated at NPT and 300 K for 10,000 timesteps of 0.2 fs after which data were collected for another 50,000 timesteps. Then, comparing the average energy of this simulation cell with the energies of the 255 water molecules without the dissolved ion plus the energy of the isolated ion gave the energy of the hydrated ion. The stepped calcite surfaces were modelled as a repeating calcite slab, containing 120 $CaCO_3$ and MCO_3 units and a gap containing the water molecules. The system was then simulated under NVT conditions. The simulation cell, consisting of calcite slab and 48 water molecules, contained 1152 species including shells.

In the DL_POLY code, the integration algorithms are based around the Verlet leap-frog scheme [44] and we used the Nosé–Hoover algorithm [45,46] for the thermostat, as this algorithm generates trajectories in both NVT and NPT ensembles, thus keeping our simulations consistent. The Nosé–Hoover parameters were set at 0.5 ps for both the thermostat and barostat relaxation times. There are two ways of treating the shells which are essentially massless; either performing an energy minimisation of shells only at each timestep [47] or assigning a small mass to the shells [48,49]. The latter is the approach used by DL_POLY. We chose 0.2 a.u. for the oxygen shell, which is small compared to the mass of the hydrogen atom of 1.0 a.u., which ensured that there would be no exchange of energy between vibrations of oxygen core and shell with oxygen and hydrogen vibrations [50]. However, due to the small shell mass, we needed to run the MD simulation with a small timestep of 0.2 fs in order to keep the system stable.

POTENTIAL MODEL

Calcite has a rhombohedral crystal structure with space group $R\bar{3}c$ and $a = b = 4.990$ Å, $c = 17.061$ Å, $\alpha = \beta = 90°$ and $\gamma = 120°$ [40]. We used the parameters for the short-range interactions derived empirically by Pavese *et al.* [42] in their study of the thermal dependence of structural and elastic properties of calcite, to model the calcite crystal and on static energy minimisation we obtained a relaxed structure of $a = b = 4.797$ Å, $c = 17.482$ Å, $\alpha = \beta = 90°$ and $\gamma = 120°$. Although Pavese *et al.*'s potential model was fitted to bulk properties, it is generally possible for ionic materials to transfer potential parameters to surface calculations. In semi-conductors, where the surface involves breaking bonds, and metals where the surface means a sudden change in the electron density, there is often a problem with transferability from bulk potential

parameters to surfaces. However, in ionic materials after relaxation, the Madelung potentials are 90% or more of the bulk values and, hence, the change of ionic radii is negligible. Oliver *et al*. [51], for example, used bulk derived potentials for their computational study comparing to scanning tunnelling microscopy results of WO_3 surfaces, and found excellent agreement between calculations and experiment. Since the surfaces considered in this work leave the carbonate group intact, the bulk derived potential model will be adequate. In addition, we showed in a previous study of the surface structures and stabilities of three calcium carbonate polymorphs, namely calcite, aragonite and vaterite, that the potential model derived by Pavese *et al*. [42] for calcite is directly transferable to different calcium carbonate phases, accurately reproducing the experimental morphologies of all three polymorphs [52].

The potential models for $MgCO_3$ and $CdCO_3$ [53] were derived to be compatible with the aforementioned calcite potential model by Pavese *et al.* [42] by fitting the parameters to reproduce the relative $MgCO_3$ and $CdCO_3$ unit cell volumes with respect to calcite and, hence, keep the experimental ratio of Ca:Cd:Mg = 1.32:1.22:1. In addition, in order to obtain reliable energies for growth of $MgCO_3$ and $CdCO_3$ onto calcite, we require the relative energies of formation to be sensible and, hence, we required the enthalpies of the following reaction to be reproduced accurately:

$$Ca^{2+}_{(g)} + MCO_{3(s)} \rightarrow M^{2+}_{(g)} + CaCO_{3(s)} \quad (1)$$

where M is either Mg or Cd. The calculated enthalpies of reaction (1) agree to within $8\,kJ\,mol^{-1}$ of the experimental enthalpies ($<3.5\%$ discrepancy) [53].

Strontianite ($SrCO_3$), spacegroup *Pmcn*, is isostructural with the aragonite phase rather than the calcite phase of $CaCO_3$, due to the larger size of the strontium ion. The $SrCO_3$ potential model, introduced in this work was, therefore, derived in a similar way to the $MgCO_3$ and $CdCO_3$ potential parameters, but relative to the aragonite structure. Again, the $SrCO_3$ potential parameters are fitted to reproduce the experimentally found relative cell volumes of Sr:Ca = 1.14:1 (from Ref. [40]) and the reaction enthalpy of the process described in Eq. (1), which was calculated for $SrCO_3$ relative to aragonite at $119.6\,kJ\,mol^{-1}$ (*cf*. exp. $122.0\,kJ\,mol^{-1}$ [54]).

The potential parameters used for the intra- and intermolecular water interactions are those described in a previous paper of MD simulations on MgO surfaces [55]. For the interactions between water molecules and calcite surfaces, we used the potential parameters previously fitted to calcite [56] and successfully used in MD simulations of water adsorption at point defects and crystal dissolution from calcite steps [25,57]. These potential parameters reproduce the

experimental heat of formation of calcite from its aqueous ions to an acceptable degree of accuracy (within 20 kJ mol^{-1}), even though the parameters were not fitted to this process. The parameters describing the interactions of the water molecules with $MgCO_3$ and $CdCO_3$ are those introduced in our study of magnesium and cadmium segregation to a variety of planar calcite surfaces [53]. As we are interested in replacing calcium by impurity cations onto the growing calcite steps, the potential parameters for $MgCO_3$ and $CdCO_3$ were fitted to reproduce accurately (to within 12 kJ mol^{-1}) the experimental enthalpies of the

TABLE I Potential parameters used in this work (short-range cutoff 10.10 Å).

Charges (e)			*Core–shell interaction* (eV Å^{-2})
Ion	Core	Shell	
Ca, Mg, Cd, Sr	+2.000		
C	+1.135		
H	+0.400		
Carbonate oxygen (O)	+0.587	−1.632	507.400000
Water oxygen (Ow)	+1.250	−2.050	209.449602
		Buckingham potential	
Ion pair	*A* (eV)	*ρ* (Å)	*C* (eV Å^6)
Ca–O	1550.0	0.29700	0.0
Ca–Ow	1186.6	0.29700	0.0
Mg–O	1092.2	0.27926	0.0
Mg–Ow	2290.0	0.22000	0.0
Cd–O	747,097.4	0.15490	0.0
Cd–Ow	3850.0	0.21500	0.0
Sr–O	1153.5	0.32200	0.0
Sr–Ow	983.1	0.27400	0.0
H–O	396.3	0.23000	0.0
H–Ow	396.3	0.25000	10.0
O–O	16,372.0	0.21300	3.47
O–Ow	12,533.6	0.21300	12.09
		Lennard–Jones potential	
	A (eV Å^{12})		*B* (eV Å^6)
Ow–Ow	39344.98		42.15
		Morse potential	
	D (eV)	*α* (Å^{-1})	r_0 (Å)
C–O	4.710000	3.80000	1.18000
H–Ow	6.203713	2.22003	0.92376
		Three-body potential	
	k (eV rad^{-2})		Θ_0
O_{core}–C–O_{core}	1.69000		120.000000
H–Ow_{shell}–H	4.19978		108.693195
		Four-body potential	
	k (eV rad^{-2})		Θ_0
C–O_{core}–O_{core}–O_{core}	0.11290		180.0
		Coulombic subtraction (%)	
$H^{0.4+}$–$O^{0.8-}$		50	
$H^{0.4+}$–$H^{0.4+}$		50	

TABLE II Calculated and experimental properties of $SrCO_3$

Property	*Calculated*	*Experimental*
Volume (Å^3)	242.1	257.0
a (Å)	4.9	5.1
b (Å)	8.1	8.4
c (Å)	6.1	6.0
$\Delta H_{\text{Eq. (1)}}$ (kJ mol^{-1})	119.6	122.0
$\Delta H_{\text{Eq. (2)}}$ (kJ mol^{-1})	−4.4	−10.1

following reaction:

$$M^{2+}_{(aq)} + CaCO_{3(s)} \rightarrow MCO_{3(s)} + Ca^{2+}_{(aq)} \quad (2)$$

where M is Cd or Mg. The parameters for the interaction of water with $SrCO_3$, introduced in this work, were fitted in exactly the same way to the process described in Eq. (2) (where M is now Sr), the enthalpy of which was then calculated at $-4.4\,\text{kJ mol}^{-1}$, in acceptable agreement with the experimental enthalpy of $-10.1\,\text{kJ mol}^{-1}$ [58]. Table I lists the parameters of the complete potential model used in this simulation study, while a comparison of calculated and experimental parameters for strontianite is made in Table II.

RESULTS

We were interested in the incorporation of impurity cations at growth steps on the dominant $(10\bar{1}4)$ surface of calcite and we, therefore, studied the $(31\bar{4}8)$ and $(3\bar{1}\,\bar{2}16)$ vicinal surfaces, which each contain $(10\bar{1}4)$ planes and monatomic steps. The steps on the $(31\bar{4}8)$ surface are acute, i.e. the carbonate groups on the edge of the step overhang the plane below the step and the angle between step wall and plane is 80° on the relaxed surface (*cf.* exp. 78° [4]). The steps on the $(3\bar{1}\,\bar{2}16)$ surface on the other hand are obtuse, i.e. the carbonate groups on the step edge lean back with respect to the $(10\bar{1}4)$ plane below with an angle between step wall and plane of 105° on the relaxed surface (exp. 102° [4]). These two types of step are found experimentally to form the edges of etch pits [4,22] and dissolution is found to occur preferentially from the obtuse step. To model aqueous conditions the stepped surfaces were covered in a monolayer of water molecules, one per surface calcium atom, which is the preferred configuration for the calcite $(10\bar{1}4)$ surface [56,59]. Previous molecular dynamics simulations of MgO surfaces in liquid water showed that there is a distinct difference in structure and density between the adsorbed monolayer and the bulk water [60] and we found that one

adsorbed monolayer of water is sufficient to mimic solvent effects and give results on calcite dissolution in acceptable agreement with experiment [25]. In previous work [25], we modelled dissolution of calcite steps, calculating the process for unhydrated and hydrated steps, and we found that only when water was included in the calculations did the calculated results agree with

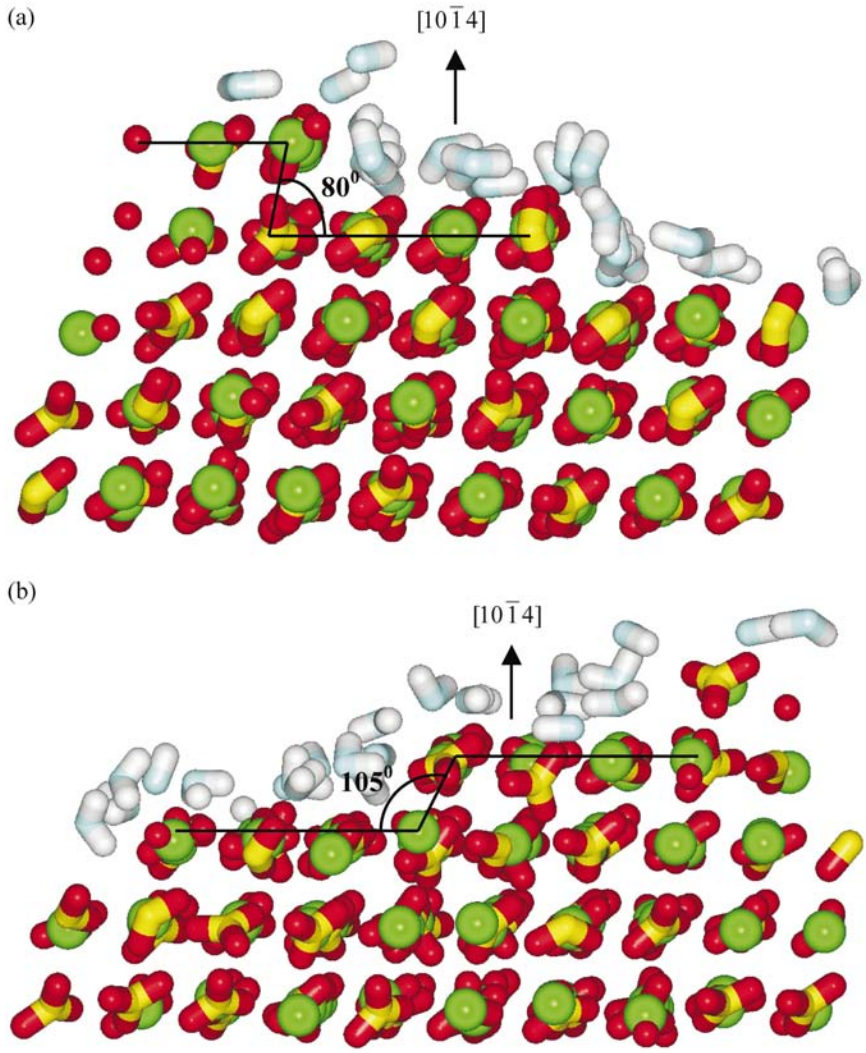

FIGURE 1 Side views of the calcite (31$\bar{4}$8) and (3$\bar{1}\bar{2}$16) surfaces, showing (10$\bar{1}$4) planes offset by (a) acute and (b) obtuse steps, with irregularly adsorbed water molecules (Ca = green, C = yellow, O = red, O_{water} = blue, H = white).

experimental findings and, hence, in this work we have only considered growth and impurity incorporation at hydrated calcite steps. The relaxed, hydrated steps are shown in Fig. 1, from which it can be seen that the water molecules do not adsorb in a regular pattern onto the surfaces, unlike the planar $(10\overline{1}4)$ surface [57], and there is some relaxation of the ions on the surface and especially at the step edge, including rotation of the carbonate groups.

We first considered growth of pure calcite at the steps, simulating the addition of successive $CaCO_3$ units to the growing edges and calculating the energy expended or released at each successive addition of a $CaCO_3$ unit. For ease of simulation, we started the calculations of a fully grown edge and removed rather than added successive $CaCO_3$ units, which ensured that the water molecules present at the surface would not overlap with added $CaCO_3$ units. After removal of a $CaCO_3$ unit, a full molecular dynamics simulation followed, whereby both the mineral surface and the adsorbed water molecules were allowed to relax to their new positions. We calculated the energies of both growth of each $CaCO_3$ unit at an isolated position on the edge and next to a unit already absorbed. In all cases, we found that growth next to an existing unit was energetically more favourable. The surfaces throughout were charge neutral and neutral $CaCO_3$ units were added to the surface, implying supersaturation conditions (at low concentrations charged units may adsorb). Having considered the stepwise growth of pure acute and obtuse calcite steps, we could then incorporate successive MCO_3 (M = Mg, Cd or Sr) units at the two steps and compare the enthalpies of decorating the calcite steps with impurity cations. Fig. 2. shows graphs of the energies expended or released upon addition of successive $CaCO_3$, $MgCO_3$, $CdCO_3$ and $SrCO_3$ units at the acute and obtuse steps, where each value on the graphs is the growth energy of adding that one particular unit, rather than an average energy. We see from the graphs, that at all stages on both the acute (Fig. 2a) and obtuse (Fig. 2b) step edges, addition of $CaCO_3$ units is energetically the least favourable process compared to addition of $CdCO_3$, $MgCO_3$ and $SrCO_3$. Initial growth of the first $CaCO_3$ unit onto both steps is the most endothermic step with the growth energies becoming less unfavourable as the steps grow until addition of the last $CaCO_3$ unit, creating another full step edge, has become exothermic. Addition of the first $CaCO_3$ unit introducing kink sites on the step is hence the rate limiting step. Growth onto the obtuse step, where the initial addition is calculated to cost $82\,kJ\,mol^{-1}$, is less energetically expensive than initial addition at the acute step ($123\,kJ\,mol^{-1}$). In addition, the second and subsequent additions of $CaCO_3$ units at the obtuse step are in each case less energetically expensive than initial growth at the acute step and, hence, on energetic grounds, $CaCO_3$ growth is predicted to occur at the obtuse rather than the acute step, in agreement with experimental findings [4].

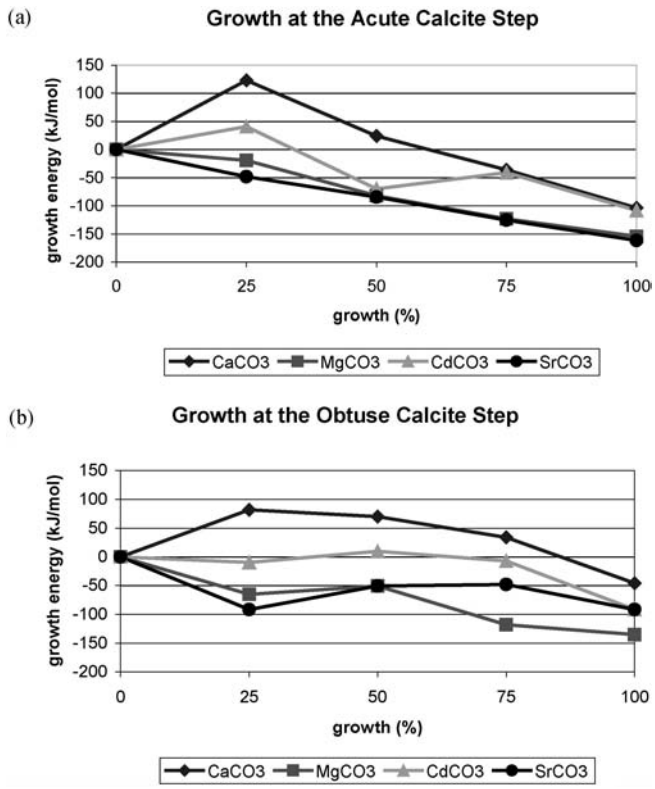

FIGURE 2 Graphs plotting the energies of addition of consecutive MCO_3 units at (a) the acute calcite step and (b) obtuse calcite edge.

Cd^{2+} is approximately the same size as Ca^{2+}, with ionic radii of 1.09 and 1.14 Å, respectively [61]. Hence, if the size of the cation is the determining factor in the addition of MCO_3 units at the step edges, we would expect $CdCO_3$ to follow a similar pattern of growth as $CaCO_3$. The curves for $CdCO_3$ in Fig. 2 are indeed similar to the $CaCO_3$ curves, although the growth energies are generally more negative. The reaction described by Eq. (2) is an exothermic process for $CdCO_3$, calculated at $-17.8\,kJ\,mol^{-1}$ (*cf.* exp. $-10.6\,kJ\,mol^{-1}$ [58]), and we might expect that the difference in growth energies between $CaCO_3$ and $CdCO_3$ would be of that order. However, from Fig. 2 we see that, apart from the last two $CdCO_3$ additions on the acute step, all $CdCO_3$ energies are more exothermic by much larger amounts of up to $90\,kJ\,mol^{-1}$ in some instances. It is, therefore, much easier to incorporate Cd^{2+} at the calcite growth edges than could be expected on purely thermodynamic grounds. Mg^{2+} (ionic radius 0.86 Å [61]) is much smaller than Ca^{2+} and as such we may expect this small cation to be easily

incorporated at both steps, although the process in Eq. (2) is endothermic for Mg^{2+} (calculated 35.2 kJ mol^{-1}, exp. 23.3 kJ mol^{-1} [58]). The graphs in Fig. 2 show that incorporation of $MgCO_3$ at the calcite steps is highly exothermic and even the initial introduction of the first $MgCO_3$ unit releases energy at both edges, indicating once again that growth at the steps is not thermodynamically controlled. Fig. 3 shows a plan view of the $(10\bar{1}4)$ surface with acute steps, decorated by magnesium ions, where for clarity, we have omitted showing the layer of water in the picture, which would otherwise obscure the surface. As

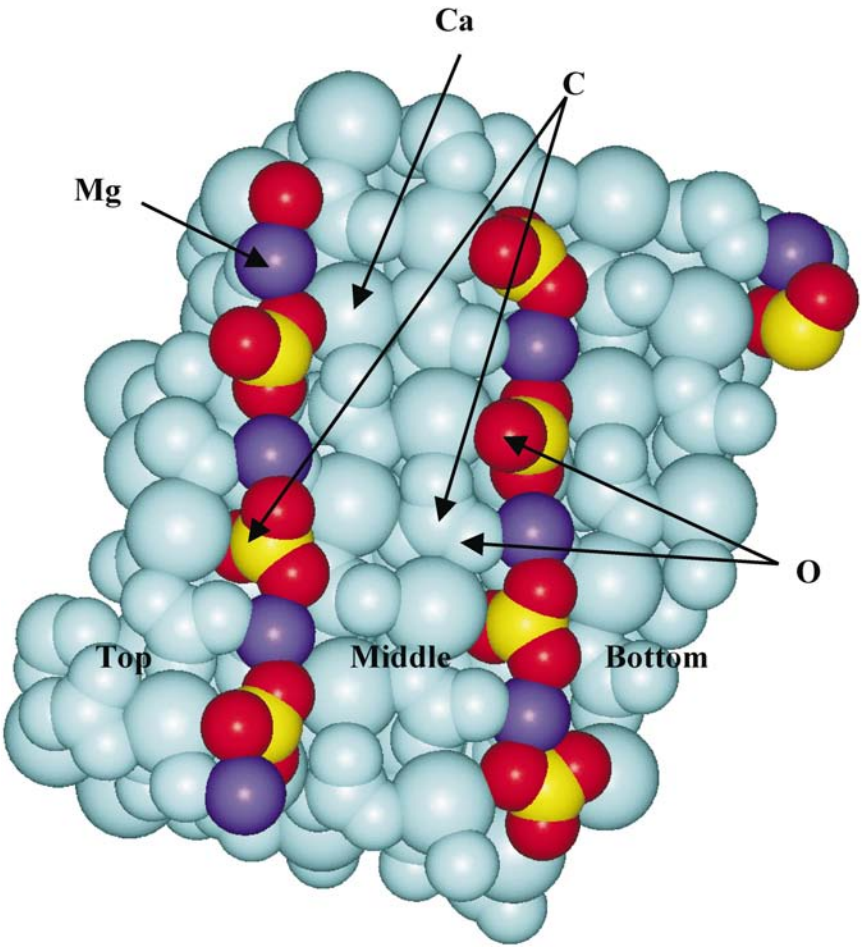

FIGURE 3 Plan view of the calcite $(31\bar{4}8)$ surface, showing acute step edges decorated by Mg^{2+} ions, where the height of the different $(10\bar{1}4)$ planes offset by the steps is indicated by "top, middle and bottom". For clarity, the water molecules are not shown (calcite crystal = pale blue, Mg = purple, C = yellow, O = red).

expected from the incorporation of a much smaller cation at the calcium sites, there is relaxation by the Mg^{2+} ions into the edge and rotation of the carbonate groups to enhance their coordination to the Mg^{2+} ions.

Finally, we investigate the incorporation of $SrCO_3$ at the two calcite steps. As mentioned above, the process of replacing calcium ions by strontium (Eq. 2) is an exothermic process, but we saw that in the case of Mg^{2+} the growth process was not dependent on the energetics of Eq. (2). Sr^{2+} (ionic radius 1.32 Å [61]) is much larger than Ca^{2+} rather than smaller as was the case for Mg^{2+}. However, the growth energies for Mg^{2+} and Sr^{2+} at the two steps are comparable, especially at the acute step. Again, incorporation of $SrCO_3$ is highly exothermic at all stages, and the energy released is much larger than the $-4.4\,kJ\,mol^{-1}$ calculated in Eq. (2).

DISCUSSION

Table III lists the average energies per added MCO_3 unit for the growth of a full edge of MCO_3 onto the acute and obtuse steps, listed in order of cation size. Growth of $CaCO_3$ units onto both steps is an endothermic process, more so at the obtuse than the acute step, even though the stepwise addition at the obtuse step is preferred due to the large energy required to form the initial kink sites on the acute step. However, growth of $(Mg,Cd,Sr)CO_3$ onto the steps is exothermic for all three carbonates. It is clear that incorporation of $MgCO_3$ at the steps releases larger energies than would be expected on thermodynamic grounds from the processes in Eq. (2). Magnesium is a small cation compared to calcium and it is incorporated as easily at the acute as at the obtuse step edge. Cadmium, which has approximately the same size as calcium, is like calcium preferentially incorporated at the acute step, although the initial addition of a $CdCO_3$ unit at the acute step edge is endothermic. The relative energies of incorporation of Mg^{2+} and Cd^{2+} instead of Ca^{2+} at the growing edge is in qualitative agreement with previous energy minimisation calculations, where we replaced Ca^{2+} by the two impurity cations on the planar $(10\bar{1}4)$ surface and found the process for Mg^{2+} to release more energy ($67.6\,kJ\,mol^{-1}$) than for Cd^{2+} ($15.4\,kJ\,mol^{-1}$) although both

TABLE III Average energies of growth of MCO_3 units onto acute and obtuse calcite steps

System	*Ionic radius* (Å)	*Eq.* (2)	*Acute step*	*Obtuse step*
$MgCO_3$	0.86	23.3	−94.7	−92.3
$CdCO_3$	1.09	−17.8	−44.7	−24.7
$CaCO_3$	1.14	0	1.8	35.0
$SrCO_3$	1.32	−4.4	−104.7	−70.6

replacement processes were exothermic. On the basis of cation size we would expect the larger Sr^{2+} ion to be preferentially incorporated at the obtuse step edge, where the cation sites are less enclosed and, therefore, more accessible to the larger ions. However, even initial growth of $SrCO_3$ is exothermic at both steps, with especially large energies released upon incorporation at the acute step edge.

There have been a number of experiments on the incorporation of impurities in growth hillocks on the $(10\bar{1}4)$ surface [19,62–64]. The vicinal surfaces of these hillocks have directions $[\bar{4}41]$ and $[48\bar{1}]$. A c glide passing through the hillock relates the four vicinal surfaces into two pairs that incorporate different impurity ions (as shown from X-ray fluorescence experiments). One pair incorporates ions with ionic radii smaller than Ca^{2+}, the other ions with ionic radii that are larger than Ca^{2+} (and also Zn^{2+}). Previous analysis of the results has been in terms of the geometry of the ideal vacuum surface. From this, it is apparent that the impurity incorporation is the result of a size effect: the larger impurities are incorporated into the more open kink site corresponding to an obtuse step, the smaller impurities are incorporated into the smaller kinks corresponding to an acute step. This, of course, ignores any effect of the solvent. Both the $(3\bar{1}\bar{2}16)$ and $(31\bar{4}8)$ surfaces are in the zone defined by the $[\bar{4}41]$ direction and are, therefore, suitable vicinal surfaces. (Since the $[\bar{4}41]$ and $[48\bar{1}]$ directions are equivalent by symmetry, our vicinal surfaces are equally suitable for the other direction as well.) Steps in the $[\bar{4}41]_+$ direction correspond to the obtuse steps; steps in the $[\bar{4}41]_-$ direction correspond to the acute steps. The calculations show that, when the effect of water is taken into account, the issue is much more finely balanced than a simple geometrical argument would suggest. Our initial calculations suggest that the incorporation of lines of impurity carbonates ($MgCO_3$, $CdCO_3$ and $SrCO_3$) at the step edge is exothermic for both acute and obtuse steps. Mg^{2+} and Cd^{2+} are preferentially incorporated into the acute step in agreement with experiment but, surprisingly, our calculations suggest that Sr^{2+} should also be incorporated into the acute step. However, the calculations to date consider only lines of impurity carbonate forming a new step edge rather than the incorporation of the impurity carbonate into an existing kink. It is clear that more detailed calculations on the incorporation of ions into the kink sites are necessary to resolve this issue. A calculation on Zn^{2+} would be particularly desirable since its behaviour is anomalous with respect to the ion size argument.

CONCLUSIONS

We have employed molecular dynamics simulations to investigate the initial stages of growth of calcium, magnesium, cadmium and strontium carbonate at

two experimentally observed calcite steps. As a result, we can make the following observations.

From the calculated energies, we expect that, in a solution containing all four cations, $MgCO_3$ and $SrCO_3$ grow onto the steps in preference to $CdCO_3$ and especially $CaCO_3$. This result is borne out by experimental evidence, which shows that the presence of magnesium ions inhibits calcite growth [26]. In addition, similar to pure calcite where the obtuse step is found to grow fastest, growth of $MgCO_3$ and $CdCO_3$ would also occur preferentially at the obtuse step edge. Initial growth of $CdCO_3$ at the obtuse calcite step is not energetically prohibited while initial incorporation of $MgCO_3$ at the obtuse step is highly exothermic, even though on average $MgCO_3$ incorporation is equally favourable at both steps. Conversely, initial $SrCO_3$ growth is highly exothermic at both steps, but very large energies are released due to growth of a complete row at the acute edge, which will, therefore, be the preferential step for incorporation of $SrCO_3$ along the complete edge.

Future work will include extending the present calculations to investigate incorporation of the impurity ions at kink sites on the edges, and also growth of $CaCO_3$ and $(Mg,Cd,Sr)CO_3$ units at the two growth steps, when they have already been decorated by the impurity cations. This will give us insight into the effect of the three cations as possible calcite growth/dissolution inducers or inhibitors.

References

[1] Beruto, D. and Giordani, M. (1993) "Calcite and aragonite formation from aqueous calcium hydrogencarbonate solutions: effect of induced electromagnetic field on the activity of $CaCO_3$ nuclei precursors", *J. Chem. Soc. Faraday Trans.* **89**, 2457.

[2] Romanek, C.S., Grossman, E.L. and Morse, J.W. (1992) "Carbon isotopic fractionation in synthetic aragonite and calcite: effects of temperature and precipitation rate", *Geochim. Cosmochim. Acta* **56**, 419.

[3] Stipp, S.L. and Hochella, M.F. (1991) "Structure and bonding environments at the calcite surface as observed with X-ray photoelectron spectroscopy (XPS) and low energy diffraction (LEED)", *Geochim. Cosmochim. Acta* **55**, 1723.

[4] Park, N.-S., Kim, M.-W., Langford, S.C. and Dickinson, J.T. (1996) "Tribological enhancement of $CaCO_3$ dissolution during scanning force microscopy", *Langmuir* **12**, 4599.

[5] Chakraborty, D. and Bhatia, S.K. (1996) "Formation and aggregation of polymorphs in continuous precipitation. 2. Kinetics of $CaCO_3$ precipitation", *Ind. Eng. Chem. Res.* **35**, 1995.

[6] Dove, P.M. and Hochella, M.F. (1993) "Calcite precipitation mechanisms and inhibition by orthophosphate: *in situ* observations by scanning force microscopy", *Geochim. Cosmochim. Acta* **57**, 705.

[7] Dreybolt, W., Eisenlohr, L., Madry, B. and Ringer, S. (1997) "Precipitation kinetics of calcite in the system $CaCO_3$–H_2O–CO_2: the conversion to CO_2 by the slow process $H^+ + HCO_3^- = CO_2 + H_2O$ as a rate limiting step", *Geochim. Cosmochim. Acta* **61**, 3897.

[8] Liu, Z. and Dreybolt, W. (1997) "Dissolution kinetics of calcium carbonate minerals in H_2O–CO_2 solutions in turbulent flow: the role of the diffusion boundary layer and the slow reaction $H_2O + CO_2 = H^+ + HCO_3^-$", *Geochim. Cosmochim. Acta* **61**, 2879.

[9] Reeder, R.J., Valley, J.W., Graham, C.M. and Eiler, J.M. (1997) "Ion microprobe study of oxygen isotopic compositions of structurally nonequivalent growth surfaces on synthetic calcite", *Geochim. Cosmochim. Acta* **61**, 5057.
[10] Zuddas, P. and Mucci, A. (1998) "Kinetics of calcite precipitation from seawater: II. The influence of the ionic strength", *Geochim. Cosmochim. Acta* **62**, 757.
[11] Chakraborty, D., Agarwal, V.K., Bhatia, S.K. and Belare, J. (1994) "Steady-state transitions and polymorph transformations in continuous precipitation of calcium carbonate", *Ind. Eng. Chem. Res.* **33**, 2187.
[12] Blanchard, D.L. and Baer, D.R. (1992) "The interactions of Co, Mn and water with calcite surfaces", *Surf. Sci.* **276**, 27.
[13] MacInnes, I.N. and Branley, S.L. (1992) "The role of dislocations and surface morphology in calcite dissolution", *Geochim. Cosmochim. Acta* **56**, 1113.
[14] Didymus, J.M., Oliver, P.M., Mann, S., De Vries, A.L., Hauschka, P.V. and Westbroek, P. (1993) "Influence of low-molecular-weight and macromolecular organic additives on the morphology of calcium carbonate", *J. Chem. Soc. Faraday Trans.* **89**, 2891.
[15] Goni, S., Sobrado, L. and Hernandez, M.S. (1993) "Increase of acid–surface reactivity through water molecules adsorption process: V_2O_5–$CaCO_3$ behaviour", *Solid State Ionics* **63**, 786.
[16] Stipp, S.L., Gutmannsbauer, W. and Lehrmann, T. (1996) "The dynamic nature of calcite surfaces in air", *Am. Mineral.* **81**, 1.
[17] Ohnesorge, P. and Binnig, G. (1993) "True atomic resolution by atomic force microscopy through repulsive and attractive forces", *Science* **260**, 1451.
[18] Liang, Y., Lea, A.S., Baer, D.R. and Engelhard, M.H. (1996) "Structure of the cleaved $CaCO_3$ $(10\bar{1}4)$ surface in an aqueous environment", *Surf. Sci.* **351**, 172.
[19] Gratz, A.J., Hillner, P.E. and Hansma, P.K. (1993) "Step dynamics and spiral growth on calcite", *Geochim. Cosmochim. Acta* **57**, 491.
[20] Hillner, P.E., Manne, S., Hansma, P.K. and Gratz, A.J. (1993) "Atomic force microscope: a new tool for imaging crystal growth processes", *Faraday Disc.* **95**, 191.
[21] Wilson, T.R.S. and Thomson, J. (1998) "Calcite dissolution accompanying early diagenesis in turbiditic deep ocean sediments", *Geochim. Cosmochim. Acta* **62**, 2087.
[22] Liang, Y., Baer, D.R., McCoy, J.M., Amonette, J.E. and LaFemina, J.P. (1996) "Dissolution kinetics at the calcite–water interface", *Geochim. Cosmochim. Acta* **60**, 4883.
[23] Liang, Y. and Baer, D.R. (1997) "Anisotropic dissolution at the $CaCO_3$ $(10\bar{1}4)$–water interface", *Surf. Sci.* **373**, 275.
[24] McCoy, J.M. and LaFemina, J.P. (1997) "Kinetic Monte Carlo investigation of pit formation at the $CaCO_3$ $(10\bar{1}4)$ surface–water interface", *Surf. Sci.* **373**, 288.
[25] de Leeuw, N.H., Parker, S.C. and Harding, J.H. (1999) "Molecular dynamics simulation of crystal dissolution from calcite steps", *Phys. Rev. B* **60**, 13792.
[26] Compton, R.G. and Brown, C.A. (1994) "The inhibition of calcite dissolution precipitation Mg^{2+} cations", *J. Colloid Interface Sci.* **165**, 445.
[27] Nassralla-Aboukais, N., Boughriet, A., Fischer, J.C., Wartel, M., Langelin, H.R. and Aboukais, A. (1996) "Electron paramagnetic resonance (EPR) study of Cu^{2+} and Mn^{2+} ions interacting as probes with calcium carbonate during the transformation of vaterite into cubic calcite", *J. Chem. Soc. Faraday Trans.* **92**, 3211.
[28] Katz, J.L., Reick, M.R., Herzog, R.E. and Parsiegla, K.J. (1993) "Calcite growth inhibition by iron", *Langmuir* **9**, 1423.
[29] Brecevic, L., Nothig-Laslo, V., Kralj, D. and Popovic, S. (1996) "Effect of divalent cations on the formation and structure of calcium carbonate polymorphs", *J. Chem. Soc. Faraday Trans.* **92**, 1017.
[30] Deleuze, M. and Brantley, S.L. (1997) "Inhibition of calcite crystal growth by Mg^{2+} at 100°C and 100 bars: influence of growth regime", *Geochim. Cosmochim. Acta* **61**, 1475.
[31] Suzuki, T., Inomata, S. and Sawada, K. (1986) "Adsorption of phosphate on calcite", *J. Chem. Soc. Faraday Trans. I* **82**, 1733.
[32] Cicerone, D.S., Regazzoni, A.E. and Blesa, M.A, (1992) "Electrokinetic properties of the calcite water interface in the presence of magnesium and organic-matter", *J. Colloid Interface Sci.* **154**, 423.
[33] Lebrón, I. and Suárez, D.L. (1996) "Calcite nucleation and precipitation kinetics as affected by dissolved organic matter at 25°C and pH >7.5", *Geochim. Cosmochim. Acta* **60**, 2765.

[34] Lebrón, I. and Suárez, D.L. (1998) "Kinetics and mechanism of precipitation of calcite as affected by $P(CO_2)$ and organic ligands at 25°C", *Geochim. Cosmochim. Acta* **62**, 405.
[35] Kenway, P.R., Oliver, P.M., Parker, S.C., Sayle, D.C., Sayle, T.X.T. and Titiloye, J.O. (1992) "Computer simulation of surface segregation", *Mol. Sim.* **9**, 83.
[36] Parker, S.C., Kelsey, E.T., Oliver, P.M. and Titiloye, J.O. (1993) "Computer modelling of inorganic solids and surfaces", *Faraday Disc.* **94**, 75.
[37] Rajam, S. and Mann, S. (1990) "Selective stabilization of the (001) face of calcite in the presence of lithium", *J. Chem. Soc. Chem. Commun.*, 1789.
[38] Hemming, N.G., Reeder, R.J. and Hart, S.R. (1998) "Growth-step-selective incorporation of boron on the calcite surface", *Geochim. Cosmochim. Acta* **62**, 2915.
[39] Nygren, M.A., Gay, D.H., Catlow, C.R.A., Rohl, A.L. and Wilson, M.P. (1998) "Incorporation of growth inhibiting diphosphonates into steps on the calcite cleavage plane surface", *J. Chem. Soc. Faraday Trans.* **94**, 3685.
[40] Deer, W.A., Howie, R.A. and Zussmann, J. (1992) Introduction to the Rock-forming Minerals (Longman, Harlow, UK).
[41] Born, M. and Huang, K. (1954) Dynamical Theory of Crystal Lattices (Oxford University Press, Oxford).
[42] Dick, B.G. and Overhauser, A.W. (1958) "Theory of the dielectric constants of alkali halide crystals", *Phys. Rev.* **112**, 90.
[43] Pavese, A., Catti, M., Parker, S.C. and Wall, A. (1996) "Modelling of the thermal dependence of structural and elastic properties of calcite, $CaCO_3$", *Phys. Chem. Miner.* **23**, 89.
[44] Forester, T.R. and Smith, W. (1995) DL_POLY User Manual (CCLRC, Daresbury Laboratory, Daresbury, Warrington, UK).
[45] Verlet, L. (1967) "Computer 'experiments' on classical fluids. I. Thermodynamical properties of Lennard–Jones molecules", *Phys. Rev.* **195**, 98.
[46] Nosé, S. (1984) "A unified formulation of the constant temperature molecular-dynamics method", *J. Chem. Phys.* **81**, 511.
[47] Hoover, W.G. (1985) "Canonical dynamics: equilibrium phase-space distributions", *Phys. Rev. A* **31**, 1695.
[48] Lindan, P.J.D. and Gillan, M.J. (1993) "Shell-model molecular dynamics simulation of superionic conduction in CaF_2", *J. Phys.: Cond. Matter* **5**, 1019.
[49] Mitchell, P.J. and Fincham, D. (1993) "Shell-model simulations by adiabatic dynamics", *J. Phys.: Cond. Matter* **5**, 1031.
[50] Ferneyhough, R., Fincham, D., Price, G.D. and Gillan, M.J. (1994) "The melting of MgO studied by molecular-dynamics simulation", *Model. Simul. Mater. Sci. Eng.* **2**, 1101.
[51] Oliver, P.M., Parker, S.C., Egdell, R.G. and Jones, F.H. (1996) "Computer simulation of the surface structures of WO_3", *J. Chem. Soc. Faraday Trans.* **92**, 2049.
[52] de Leeuw, N.H. and Parker, S.C. (1998) "Surface structure and morphology of calcium carbonate polymorphs calcite, aragonite and vaterite: an atomistic approach", *J. Phys. Chem. B* **102**, 2914.
[53] de Leeuw, N.H. and Parker, S.C. (2000) "Modeling absorption and segregation of magnesium and cadmium ions to calcite surfaces: introducing $MgCO_3$ and $CdCO_3$ potential models", *J. Chem. Phys.* **112**, 4326.
[54] Lide, D.R. (2000) CRC Handbook of Chemistry and Physics (CRC, Boca Raton).
[55] de Leeuw, N.H. and Parker, S.C. (1998) "Molecular-dynamics simulation of MgO surfaces in liquid water using a shell-model potential model for water", *Phys. Rev. B* **58**, 13901.
[56] de Leeuw, N.H. and Parker, S.C. (1997) "Atomistic simulation of the effect of molecular adsorption of water on the surface structure and energies of calcite surfaces", *J. Chem. Soc. Faraday Trans.* **93**, 467.
[57] de Leeuw, N.H. and Parker, S.C. (2000) "Atomistic simulation of mineral surfaces", *Mol. Simul.* **24**, 71.
[58] Weast, R.C. and Astle, M.J. (1981) CRC Handbook of Chemistry and Physics (CRC, Boca Raton).
[59] de Leeuw, N.H., Redfern, S.E. and Parker, S.C. (1998) Recent Research Developments in Physical Chemistry 2 (Transworld Research Network, Trivandrum, India) **2**.
[60] de Leeuw, N.H., Watson, G.W. and Parker, S.C. (1996) "Atomistic simulation of adsorption of water on three-, four- and five-coordinated surface sites of magnesium oxide", *J. Chem. Soc. Faraday Trans.* **92**, 2081.

[61] Shannon, R.D. (1976), *Acta Cryst. A* **32**, 751.
[62] Paquette, J. and Reeder, R.J. (1990) "New type of compositional zoning in calcite: insights into crystal-growth mechanisms", *Geology* **18**, 1244.
[63] Paquette, J. and Reeder, R.J. (1995) "Relationship between surface structure, growth mechanism and trace element incorporation in calcite", *Geochim. Cosmochim. Acta* **59**, 735.
[64] Reeder, R.J. (1996) "Interaction of divalent cobalt, zinc, cadmium and barium with the calcite surface during layer growth", *Geochim. Cosmochim. Acta* **60**, 1543.